Journal of Organometallic Chemistry, 449 (1993) 173–180

JOM 23366

Studies of the thermal and photochemical lability of olefin complexes of rhodium(I) to form Rh and Rh_2O_3

Zhibang Duan and Mark J. Hampden-Smith

Department of Chemistry and Center for Micro-Engineered Ceramics University of New Mexico, Albuquerque NM 87131 (USA)

Alan P. Sylwester

Department 6211, Sandia National Laboratory, Albuquerque NM 87185 (USA)

(Received September 3, 1992)

Abstract

Thermogravimetric analyses of the series of compounds $[L_2RhCl]_2$, where L_2 = 1,5-COD, NBD and $(C_2H_4)_2$ under air, nitrogen and 7%H_2 in N_2 atmospheres reveal that thermal decomposition behavior depends on the nature of the olefin ligand and the composition of the atmosphere. Under a 7% H_2 in N_2 atmosphere, the onset of thermal decomposition of these species occurs in the following order: $L_2 = (C_2H_4)_2$, 91°C; NBD, 143°C; 1,5-COD, 212°C. Under a nitrogen atmosphere, $[L_2RhCl]_2$, L_2 = NBD and $(C_2H_4)_2$, undergo weight loss consistent with loss of one or more olefin ligands, then formation of Rh metal at higher temperatures. In contrast, $[(1,5\text{-COD})RhCl]_2$ formed Rh metal directly. In air, thermal decomposition generally resulted in formation of crystalline Rh metal followed by oxidation above 500°C to form crystalline Rh_2O_3, except for $[(C_2H_4)_2RhCl]_2$, which gave Rh_2O_3 directly. The Rh and Rh_2O_3 powders were analyzed by powder X-ray diffraction. In some experiments, a weight loss consistent with formation of "RhCl" was observed. However, as a result of the crystalline Rh present, it is proposed that disproportionation to Rh and $RhCl_3$ may have occurred.

The compound $[(C_2H_4)_2Rh(OEt)]_2 \cdot H_2O$ is photolabile and undergoes decomposition on exposure to UV radiation to give crystalline, 2 nm sized Rh metal particles as determined by TEM, EDS and electron diffraction.

1. Introduction

A variety of methods for the synthesis of highly dispersed metal particles has been investigated, including chemical reduction, decomposition of organometallic compounds and metal atom vapor synthesis [1,2]. The advantages and disadvantages of these techniques as methods for the formation of supported catalysts were recently reviewed [1]. One of the advantages of using organometallic compounds as precursors for formation of highly dispersed metals is their low thermal decomposition temperature [3]. In heterogeneous catalysis applications, the active metal is normally dispersed on a metal oxide support such as SiO_2 or TiO_2. Preparation methods such as impregnation, co-precipitation and ion exchange generally require calcination and reduction processes [4]. During the calcination process, the metal is normally oxidized to form the metal oxide which aids removal of the organic ligands by their oxidation [5]. This is usually followed by a reduction step in which the metal oxide is reduced to form the active metal dispersed on the metal oxide support. However, the relatively high temperature required for these steps [5,6] can cause aggregation of the final metal catalyst particles, resulting in changes in size-dependent properties such as activity and selectivity [7] and can also lead to changes in the microstructure (surface area, porosity) of the metal oxide support [8]. Therefore, low temperature routes to highly dispersed metal particles are desirable to circumvent these problems.

Many groups have studied the formation of highly dispersed rhodium particles derived from inorganic and organometallic precursors either as colloidal solutions or supported on metal oxide supports for their catalytic hydrogenation activity. Rhodium(III) com-

Correspondence to: Dr. M.J. Hampden-Smith.

0022-328X/93/$6.00

pounds are commonly used, including $Rh(allyl)_3$ and $RhCl_3$ [4,9]. Rhodium(I) compounds can be reduced directly under a variety of atmospheres at low temperatures to form metallic rhodium. For example, the thermal decomposition of $[\{(1,5\text{-COD})Rh\}_2Sn(OEt)_6]$ in air yields Rh and SnO_2 [10] while reaction of this species with silica spheres followed by thermolysis at 200°C under hydrogen results in formation of highly dispersed, 24 Å-sized rhodium/tin alloy particles on the silica surface [11]. Similarly, the addition of hydrogen to hydrocarbon solutions of $[(1,5\text{-COD})RhH]_4$ at room temperature and pressure results in formation of 2 nm sized, crystalline rhodium particles [12,13].

Several approaches to the formation of rhodium films via chemical vapor deposition, (CVD) of Rh^I and Rh^{III} organometallic compounds have been described. The CVD of $Rh(allyl)_3$ in H_2 at atmospheric pressure resulted in formation of amorphous Rh films at substrate temperatures as low as 120°C [14]. The plasma-enhanced (PE) CVD of $Rh(CO)_2(acac)$, where acac = acetylacetonate, resulted in 98% pure Rh films in the presence of atomic hydrogen at substrate temperatures of 150°C [15]. Remote plasma CVD studies using $Rh(allyl)_3$ produced > 97% pure Rh films in the presence of $H\cdot$, but CVD in the presence of H_2 resulted in considerable (14%) carbon contamination [16].

The work reported here focuses on developing an understanding of the conditions under which Rh metal can be formed under mild conditions from organometallic precursors. In this work, we report the results of a study of the thermolysis and photolysis behavior of a series of common olefin complexes of Rh^I under hydrogen, nitrogen, and air atmospheres. The data show that hydrogen reduction generally results in the formation of rhodium metal under mild conditions (~ 200°C) while thermolysis in air is consistent with the loss of the olefin ligand followed by reduction to give rhodium metal which on further heating in air oxidizes to form crystalline Rh_2O_3. Photolysis of $[(C_2H_4)_2Rh(OEt)]_2\cdot H_2O$ results in the smooth formation of small rhodium particles at room temperature.

2. Experimental details

2.1. General procedures

All manipulations were carried out under an atmosphere of dry nitrogen using standard Schlenk techniques [17]. All hydrocarbon and ethereal solvents were dried and distilled from sodium benzophenone ketyl and stored over 4 Å molecular sieves under a nitrogen atmosphere prior to use. The olefins, 1,5-COD, NBD (where 1,5-COD = 1,5-cyclooctadiene and NBD = 2,5-norbornadiene) and ethylene, were purchased from Aldrich Chemical Company. The compound $RhCl_3\cdot 3H_2O$ was obtained via the Johnson-Matthey precious metals loan program and converted to $[(1,5\text{-COD})RhCl]_2$, $[(NBD)RhCl]_2$ and $[(C_2H_4)_2RhCl]_2$ by the literature methods [18–20]. The integrity of these compounds was confirmed by elemental analysis, FT-IR, ^1H and ^{13}C NMR spectroscopy.

Elemental analysis were performed by Ms. R. Ju at the Department of Chemistry, University of New Mexico. NMR data were recorded on a Bruker AC-250P NMR spectrometer using the protio impurities of the deuterated solvents as references for the ^1H NMR, and the ^{13}C resonance of the solvents as reference for ^{13}C NMR spectroscopy. Temperatures were calibrated with either ethylene glycol or methanol. IR data were recorded on a Perkin-Elmer Model 1620 FTIR spectrophotometer. Mass spectra were recorded on a Finnegan GC-mass spectrometer. Thermogravimetric analysis was carried out on a Perkin-Elmer TGA-7 Thermogravimetric Analyzer with a heating rate of 10 deg/min in static air, N_2 and 7% H_2/N_2 atmospheres with a flow rate of 190 ml/min. Analytical data for $[(C_2H_4)Rh_2Cl_2]$ isolated from thermolysis of $[(C_2H_4)_4Rh_2Cl_2]$ at 175°C: Found: C, 7.67; H, 1.06; Calcd.: C, 7.88; H, 1.32%.

2.2. Synthesis of $[(C_2H_4)_2Rh(OEt)]_2\cdot H_2O$

This synthesis was carried out in the absence of light under a nitrogen atmosphere. $[(C_2H_4)_2RhCl]_2$, 0.80 g (2.06 mmol), and 0.196 g (4.90 mmol) of NaOH were added to 100 ml of ether in an ice and salt bath. To this suspension, 8 ml of degassed ethanol was added. The reaction mixture was stirred for 2 h, and the volatile components were removed *in vacuo*. The crude product was extracted by 6 × 10 ml of a mixture of benzene and pentane solvent (~ 5:2) at 0°C. The extractant was kept in an ice and salt bath. After removing the volatile components *in vacuo*, 0.53 g of yellow product was obtained at a yield of 60%. Elemental analysis: Found: C, 33.94; H, 6.79; $C_{12}H_{28}O_3Rh_2$ calcd: C, 33.82; H, 6.62%.

IR data (KBr disk, cm^{-1}): 3584.7vs, 3450.9vs, br, 3053.0m, 2989.5m, 1635.1w, 1511.9m, 1436.8m, 1223.5,s, 1214.1s, 1053.5m, 979.5s, 507.1w, 416.7s. ^1H NMR (C_6D_6, 20°C, 250 MHz) δ (ppm): 2.59 (q, 4H, 2 CH_2, J 6.8 Hz), 2.21 (br s, *16H*, 8 CH_2), 0.98 (t, 6H, 2 CH_3, J 6.8 Hz). $^{13}C\{^1H\}$ NMR (C_6D_6, 20°C, 62.9 MHz) δ (ppm): 55.2 (d, C_2H_4, J (Rh–C) 14.5 Hz), 54.4 (s, CH_2), 21.1 (s, CH_3). Variable temperature ^1H NMR (C_7D_8, 250 MHz) δ (ppm): 50°C, 2.62 (q, CH_2, J 6.7 Hz), 2.23 (br s, C_2H_4), 0.98 (t, CH_3, J 6.7 Hz); 40°C, 2.60 (q, CH_2, J 6.7 Hz), 2.22 (br s, C_2H_4), 0.98 (t, CH_3, J 6.7 Hz); 20°C, 2.57 (q, CH_2, J 6.7 Hz), 2.17 (br s, C_2H_4), 0.97 (t, CH_3, J 6.8 Hz); 15°C, 2.57 (q, CH_2, J

6.8 Hz), 2.16 (br s, C_2H_4), 0.97 (t, CH_3, J 6.8 Hz); 10°C, 2.56 (q, CH_2, J 6.8 Hz), 2.17 (br s, C_2H_4), 1.88 (br s, C_2H_4), 0.97 (t, CH_3, J 6.8 Hz); 0°C, 2.68 (br s, C_2H_4), 2.53 (q, CH_2, J 6.8 Hz), 1.75 (br s, C_2H_4), 0.97 (t, CH_3, J 6.8 Hz); −20°C, 2.70 (d, C_2H_4, ^2J (Rh–H) 12.4 Hz), 2.52 (q, CH_2, J 6.8 Hz), 1.73 (d, C_2H_4, ^2J (Rh–H) 12.4 Hz), 0.97 (t, CH_3, J 6.8 Hz); −60°C, 2.71 (d, C_2H_4, ^2J (Rh–H) 12.8 Hz), 2.47 (q, CH_2, J 6.8 Hz), 1.72 (d, C_2H_4, ^2J (Rh–H) 12.8 Hz), 0.97 (t, CH_3, J 6.8 Hz). T_c = 285 K. $\Delta G_c^\dagger$ = 13.1 Kcal mol^{-1}.

Variable temperature ^{1}H NMR (C_7D_8, 250 MHz) for $[(C_2H_4)_2RhCl]_2$ δ (ppm): 20°C, 2.82 (br s); 10°C, 2.82 (br s); 0°C, 2.82 (br s); −5°C, 3.3 (br s), 2.4 (br s); −20°C, 3.64 (br s), 1.98 (br s); −40°C, 3.67 (br s), 1.96 (br s); −60°C, 3.72 (d, ^2J (Rh–H) 13.3 Hz), 1.91 (d, ^2J (Rh–H) 13.3 Hz). ^{13}C {^{1}H} NMR (C_7D_8, 62.9 MHz) δ (ppm): −60°C, 60.7 (d, C_2H_4, J (Rh–C) 13.3 Hz). T_c = 268 K. $\Delta G_c^\dagger$ = 12.0 Kcal mol^{-1}.

2.3. Photolysis experiments

The compound $[(C_2H_4)_2RhOEt]_2 \cdot H_2O$, 0.015 g (0.035 mmol) was dissolved in 0.6 ml of benzene-d_6 in a 5 mm NMR tube. The solution was irradiated with a mercury lamp at room temperature, and ^{1}H NMR spectra were measured at various times.

For a larger scale experiment, 0.060 g (0.141 mmol) of $[(C_2H_4)_2RhOEt]_2 \cdot H_2O$ was dissolved in 10 ml of benzene in a 50 ml Schlenk flask. Then the solution was irradiated with a mercury lamp for 4 h at room temperature. The volatile components were removed *in vacuo*, and 0.029 of black powder was obtained in quantitative yield. The identity of the black powder was confirmed to be rhodium by energy dispersive spectroscopy (EDS) and X-ray powder diffraction (XRD).

2.4. Characterization of rhodium particles

Scanning electron microscopy was carried out on a Hitachi S-800 instrument. The rhodium particles were examined in a JEOL 2000-FX transmission electron microscope operating at 200 KeV by suspending the particles on porous carbon films supported on a 3 mm Cu grid. Elemental analysis was performed using a Tracor Northern 5500 energy dispersive X-ray analyzer with the microscope operated in S mode.

3. Results and discussion

3.1. Syntheses and characterization

The compounds $[L_2RhCl]_2$ where L_2 = 1,5-COD, NBD and $(C_2H_4)_2$ were prepared according to literature methods [18–20] and gave satisfactory spectroscopic and analytical data. The compound $[(C_2H_4)_2Rh(OEt)]_2 \cdot H_2O$ was prepared by the reaction of $[(C_2H_4)_2RhCl]_2$ with sodium hydroxide in ethanol with reasonable yield (60%). Satisfactory elemental analytical data were obtained, and the strong bands attributed to ν(O–H) in the IR spectrum are consistent with the presence of a water molecule of crystallization. NMR spectroscopic data were consistent with $[(C_2H_4)_2Rh(OEt)]_2$, but no ^{1}H NMR peaks that could be attributed to water were observed. The compound $[(C_2H_4)_2Rh(OEt)]_2 \cdot H_2O$ was found to be quite photochemically and thermally labile (room light and room temperature for long periods). It was best stored in the dark at low temperature. For both $[(C_2H_4)_2RhCl]_2$ and $[(C_2H_4)_2Rh(OEt)]_2 \cdot H_2O$, the ethylene ligands gave rise to a single, broad ^{1}H NMR resonance at room temperature, indicative of a dynamic exchange process. It has been shown that, in the solid state structure of $[(C_2H_4)_2RhCl]_2$, the ethylene double bond is oriented perpendicular to the coordination plane [21]. The orientation of the olefin ligand perpendicular to the square planar coordination environment about Rh is a general structural feature of $[L_2RhCl]_2$ species. In solution, however, the coordinated ethylene molecules rotate about the olefin metal bond axis, as determined by variable temperature ^{1}H NMR. This phenomenon has been demonstrated for $(\eta^5$-$C_5H_5)Rh(C_2H_4)_2$ [22].

At 20°C, the ^{1}H NMR spectrum of $[(C_2H_4)_2RhCl]_2$ in toluene-d_8 exhibited only a broad peak at 2.82 ppm. When the solution was cooled to −20°C, two separate broad peaks centered at 3.64 and 1.98 ppm were observed, which resulted from the two chemically and magnetically inequivalent protons on ethylene [22]. On further cooling to −60°C, both peaks were split into doublets due to rhodium coupling (^2J(Rh–H) = 13.3 Hz). At −5°C, the two peaks coalesced. The free energy of activation, $\Delta G_c^\dagger$, calculated on the basis of these data [23], was found to be 12.0 (+/− 0.5) Kcal mol^{-1}.

The complex $[(C_2H_4)_2Rh(OEt)]_2 \cdot H_2O$ exhibited a similar phenomenon. At 20°C the ^{1}H NMR spectrum of $[(C_2H_4)_2RhOEt]_2 \cdot H_2O$ in toluene-d_8 showed only a broad peak at 2.17 ppm for the ethylene protons. At 0°C this peak was displaced by two separate broad peaks at 2.68 and 1.75 ppm derived from the slow rotation of the coordinated ethylene molecules compared to the ^{1}H NMR timescale. At −60°C, both of the peaks were split into doublets by rhodium coupling with ^2J(Rh–H) = 12.4 Hz. The activation free energy ($\Delta G_c^\dagger$) was calculated to be 13.1 (+/− 0.5) Kcal mol^{-1}. It is interesting to note that the $\Delta G_c^\dagger$ values for the two compounds are consistent with the ^1J(Rh–C) coupling constant data of 14.5 Hz for $[(C_2H_4)_2Rh(OEt)]_2 \cdot H_2O$ and 13.3 Hz for $[(C_2H_4)_2RhCl]_2$, where the ^1J(Rh–C) coupling constant is larger for the compound with the

TABLE 1. Thermogravimetric data of the studied complexes

Complexes	Atmosphere	Range of decomposition temp. (°C)	Peak temperature of DTG (°C)	Proposed decomposition products	Loss of weight (%)	
					Calcd.	Found
$[(COD)RhCl]_2$	7% H_2/N_2	170–273	252	Rh	58.26	58.2
	N_2	270–348	325	Rh	58.26	58.4
	Air	224–320	293	RhCl	43.88	44.8
		336–360	354	Rh	58.26	60.3
		480–580	523	Rh_2O_3	48.53	52.4
$[(NBD)RhCl]_2$	7% H_2/N_2	130–193	158	Rh	55.36	56.5
	N_2	180–295	282	$(NBD)Rh_2Cl_2$ [a]	19.99	21.1
		295–460	348	RhCl	39.07	38.0
	Air	226–370	242, 276, 313, 358	$(NBD)Rh_2Cl_2$ [a]	19.99	21.1
		370–425	411	Rh	55.36	55.8
		500–620	552	Rh_2O_3	44.94	47.3
$[(C_2H_4)_2RhCl]_2$	7% H_2/N_2	86–179	97	Rh	47.08	47.3
	N_2	126–174	157	$(C_2H_4)Rh_2Cl_2$ [b]	21.64	20.4
		174–355	237, 310	Rh	47.08	44.8
	Air	137–168	156	$(C_2H_4)Rh_2Cl_2$ [b]	21.64	21.5
		212–400	352	RhCl	28.85	26.9
		590–700	659	Rh_2O_3	34.74	35.0

[a] Composition based on observed weight loss. [b] Composition based on elemental analysis data.

higher barrier to exchange. However, the ^2J(Rh–H) coupling constants exhibit the opposite trend.

3.2. *Thermal stability of $[L_2RhCl]_2$ L = olefin complexes*

The results of the thermogravimetric analysis (TGA) study of the compounds $[L_2RhCl]_2$ where L_2 = 1,5-COD, NBD and $(C_2H_4)_2$ under nitrogen, 7% hydrogen in nitrogen, and air atmospheres are summarized in Table 1. TGA data for a representative example are presented in Figs. 1 and 2. Figure 1 shows a comparison of the TGA data for $[(COD)RhCl]_2$ in air, nitrogen and 7% hydrogen in nitrogen atmospheres. Figure 2 shows a comparison of the TGA data for all three compounds under the same atmosphere, 7% nitrogen in hydrogen. The complexes undergo different decomposition processes depending on the nature of the olefin ligand and the atmosphere.

In static air, $[(1,5\text{-COD})RhCl]_2$ underwent a weight loss that corresponded to liberation of 1,5-COD in the temperature region 224–320°C, resulting in formation of a residue with empirical formula, "RhCl", see Fig. 1. Further heating resulted in another weight loss that

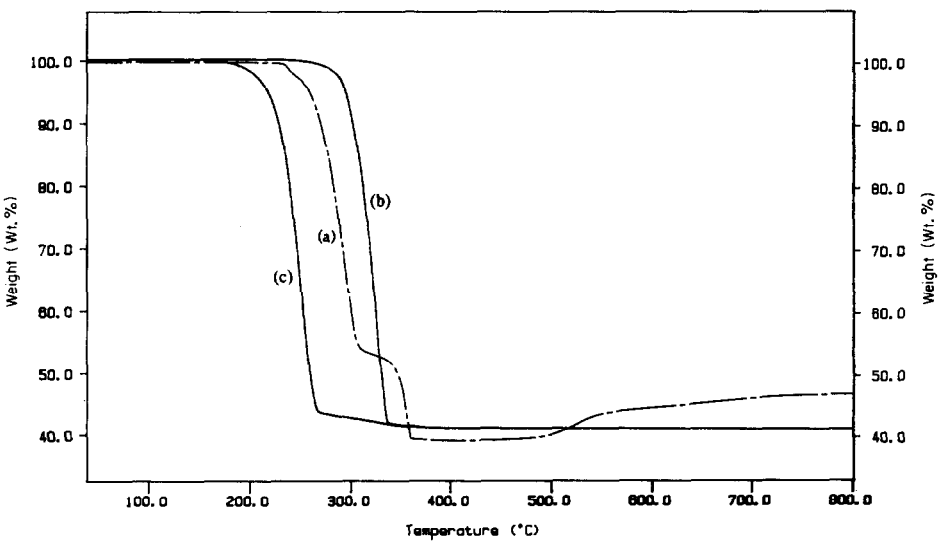

Fig. 1. TGA curves of $[(1,5\text{-COD})RhCl]_2$, heated under three different atmospheres: (a) air, (b) N_2, (c) 7% H_2/N_2.

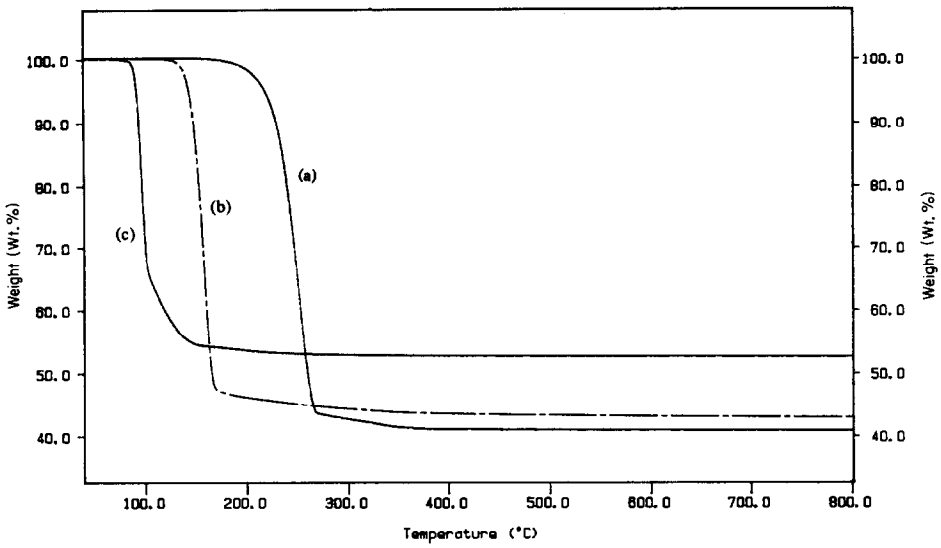

Fig. 2. TGA data for (a) $[(1,5\text{-COD})RhCl]_2$, (b) $[(NBD)RhCl]_2$ and (c) $[(C_2H_4)_2RhCl]_2$ heated in 7% H_2/N_2.

corresponded to loss of Cl · and formation of Rh. The TGA curve remained flat over the region 360–480°C. On further heating above 480°C in air, a weight gain was observed consistent with formation of Rh_2O_3. To investigate these qualitative observations further, thermal decomposition experiments were conducted separately on a larger scale. Thermolysis of $[(1,5\text{-COD})RhCl]_2$ in static air at 300°C resulted in a weight loss that corresponded to loss of 1,5-COD. Thermogravimetric analysis of the product formed was carried out, and a loss of 25.7% in weight between 271 and 425°C was observed, which matches the theoretical value of 25.62% for the decomposition of "RhCl" to Rh metal. However, X-ray powder diffraction data for the species isolated after loss of 1,5-COD revealed the presence of crystalline Rh metal. It is therefore likely that "RhCl" may have disproportionated to give $RhCl_3$ and Rh, although crystalline $RhCl_3$ was not observed. Disproportionation has recently been proposed in the thermal decomposition of $[(F_3P)_2RhCl]_2$ according to the equation below [24].

$$3[(F_3P)_2RhCl]_2 \longrightarrow 4Rh + 2RhCl_3 + 12PF_3$$

In another experiment, $[(1,5\text{-COD})RhCl]_2$ was heated to 320°C and cooled to room temperature. The formation of crystalline Rh metal was confirmed by X-ray powder diffraction data as shown in Fig. 3. On further heating in air, the rhodium metal was oxidized to form crystalline Rh_2O_3, as determined by X-ray powder diffraction data, as shown in Fig. 4. This demonstrates that there are conditions under which this species can be reduced directly to Rh metal without the need for oxidation to remove the organic supporting ligands.

Under N_2 gas, $[(1,5\text{-COD})RhCl]_2$ decomposes in a single step to form rhodium metal as determined by TGA data and X-ray powder diffraction data. Similarly, Rh metal is formed in a single step in a 7% H_2/N_2 atmosphere. However, the decomposition temperature is much lower in 7% H_2/N_2 atmosphere than that in N_2 gas and in static air. This is also true for the other two complexes. $[(NBD)RhCl]_2$ and $[(C_2H_4)_2RhCl]_2$. The oxidative addition of hydrogen to the Rh center, followed by reductive elimination of the alkane, may play an important role in the decomposition of the complexes under a hydrogen atmosphere. Hydrogenation of olefin ligands have previously been reported as byproducts [10].

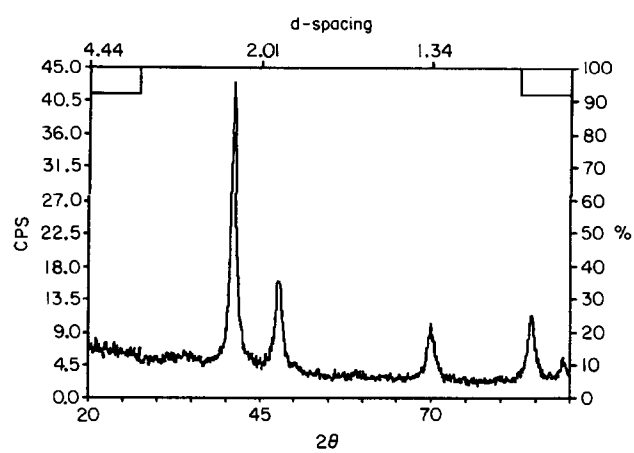

Fig. 3. X-ray powder diffraction data for the powder obtained on heating $[(1,5\text{-COD})RhCl]_2$ at 372°C for 1 h. Only peaks due to Rh were observed.

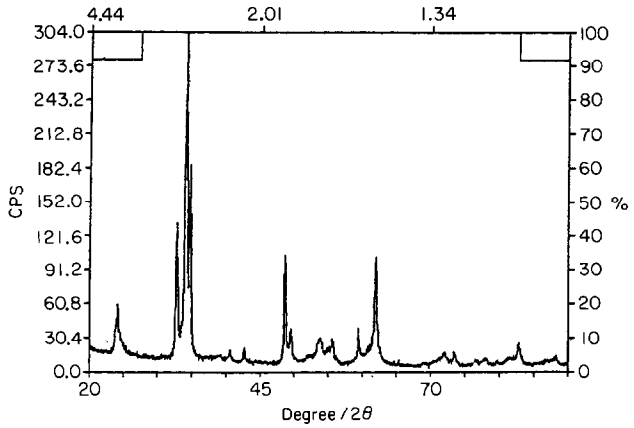

Fig. 4. X-ray powder diffraction data for the powder obtained on heating $[(1,5\text{-COD})RhCl]_2$ to 1000°C. Only peaks due to Rh_2O_3 were observed.

$[(NBD)RhCl]_2$ decomposes in static air (Table 1) via several thermally unstable intermediates to give rhodium metal. On the derivative curve, there are four peaks in the temperature region of 226–370°C, which correspond to the decomposition of the intermediates. Rhodium is oxidized to form Rh_2O_3 above 500°C. Under a N_2 atmosphere, $[(NBD)RhCl]_2$ undergoes a weight loss that corresponds to loss of one NBD ligand and subsequently decomposes further consistent with formation of "RhCl" (see Table 1). Analogous to $[(1,5\text{-COD})RhCl]_2$, $[(NBD)RhCl]_2$ decomposes in one step to give Rh metal under 7% H_2/N_2 atmosphere.

In contrast to $[(1,5\text{-COD})RhCl]_2$ and $[(NBD)RhCl]_2$, thermal decomposition of $[(C_2H_4)_2RhCl]_2$ in static air resulted in a weight loss that corresponded to loss of three ethylene ligands to form a species with empirical formula "$(C_2H_4)Rh_2Cl_2$", as confirmed by elemental analysis, in the region of 137–168°C. On continued heating, further weight loss was observed, corresponding to formation of "RhCl" (which may be Rh and $RhCl_3$ as described above) in the temperature range 212°C to 400°C. "RhCl" decomposed to form Rh_2O_3 in the temperature range 590–700°C.

Under N_2 atmosphere, $[(C_2H_4)_2RhCl]_2$ undergoes a weight loss again corresponding to loss of three of four ethylene ligands between 126 and 174°C. However, the intermediate complex decomposes to form rhodium metal. Under 7% H_2/N_2 gas, $[(C_2H_4)_2RhCl]_2$ decomposes in one step to form Rh metal (see Fig. 2).

From the above results, it can be seen that the olefin ligands greatly affect the thermal stability and the decomposition pathway in these complexes. Generally, the thermal stability of the three complexes studied decreased in the order: $[(1,5\text{-COD})RhCl]_2 > [(NBD)RhCl]_2 > [(C_2H_4)_2RhCl]_2$, as judged by the onset of weight loss and the temperature at which Rh is formed under mixed H_2/N_2 and N_2 atmospheres. In a hydrogen atmosphere, the complexes decompose in a single step to give rhodium metal. However, in static air and nitrogen gas, the complexes show different behavior depending on the olefin ligands.

It is possible to calculate the activation energy of the thermal decomposition reaction and the reaction order directly from the TGA data [25]. Under a nitrogen atmosphere, the TGA data were used to calculate the activation energies for the conversion of $[(1,5\text{-COD})RhCl]_2$ to Rh metal (46.5 Kcal mol^{-1}), $[(NBD)RhCL]_2$ to $(NBD)Rh_2Cl_2$ (47.0 Kcal mol^{-1}), and $[(C_2H_4)_2RhCl]_2$ to $(C_2H_4)Rh_2Cl_2$ (60.8 Kcal mol^{-1}). The reaction order for the three complexes is approximately 1. However, these numbers do not reflect the trends in activation barrier expected based on the onset temperatures observed under identical conditions. This is probably because each weight loss corresponds to a different reaction, and the activation energies do not represent the same fundamental steps.

3.3. *Photolysis of* $[(C_2H_4)_2RhOEt]_2 \cdot H_2O$ *and* $[(C_2H_4)_2RhCl]_2$

Photolysis of benzene solutions of $[(1,5\text{-COD})RhCl]_2$ and $[(NBD)RhCl]_2$ with a mercury arc lamp did not lead to any observed change in 2 h. Photolysis of benzene solutions of $[(C_2H_4)_2RhCl]_2$ resulted in slow formation of a black powder and a black mirror on the walls of the reaction vessel. Scanning electron microscopy of the black deposit on the reaction vessel walls revealed the presence of agglomerated ~ 0.1 μm-sized particles, as shown in Fig. 5, which contained Rh as determined by energy dispersive spectroscopy. However, distinction between the presence of rhodium metal and other rhodium containing products such as rhodium oxide was not possible.

Irradiation of dilute benzene-d_6 solutions of $[(C_2H_4)_2Rh(OEt)]_2 \cdot H_2O$ were monitored as a function of time by ^1H NMR spectroscopy. Rapid disappearance of the starting material was observed, together with concomitant formation of ethylene, ethanol, ethane and acetaldehyde. At the same time, the solution darkened, and a black powder was precipitated. This reaction was complete in less than 10 min of irradiation.

By irradiating a concentrated benzene solution of this compound on a larger scale, a black colloid was produced and a metallic mirror was formed on the walls of the reaction vessel. The metallic mirror deposited on the reaction vessel wall was removed with a spatula and characterized by SEM and EDS. The powder obtained in this way consisted of spherical particles which were essentially monodispersed with diameters of approximately 0.4 μm, as shown in Fig. 6.

Fig. 5. SEM of powder deposited on the reaction vessel walls upon photolysis of $[(C_2H_4)_2RhCl]_2$ for 8 h.

To gain further insight, a TEM study of the contents of the solution formed after photolysis of $[(C_2H_4)_2Rh(OEt)]_2 \cdot H_2O$ for 25 min was carried out. TEM of the sample revealed the presence of monodispersed 2 nm sized particles (see Fig. 7). Electron diffraction experiments on these particles revealed a single diffuse ring with a d-spacing of 2.2 Å, consistent with that of face-centered cubic rhodium metal.

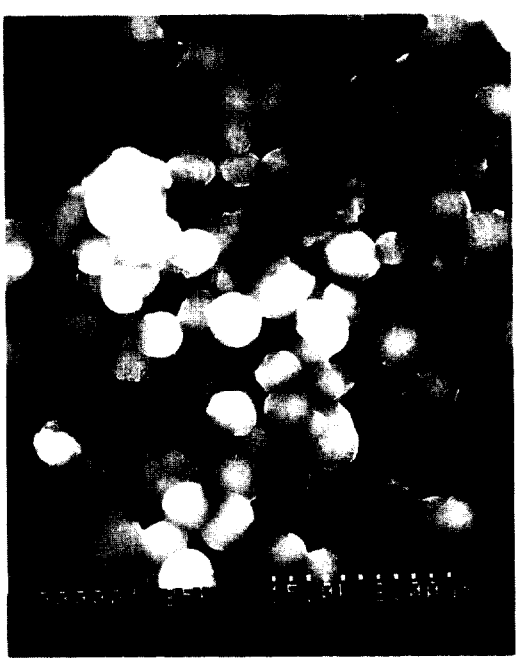

Fig. 6. SEM of the powder deposited on the reaction vessel walls upon photolysis of $[(C_2H_4)_2RhOEt]_2$ for 25 min.

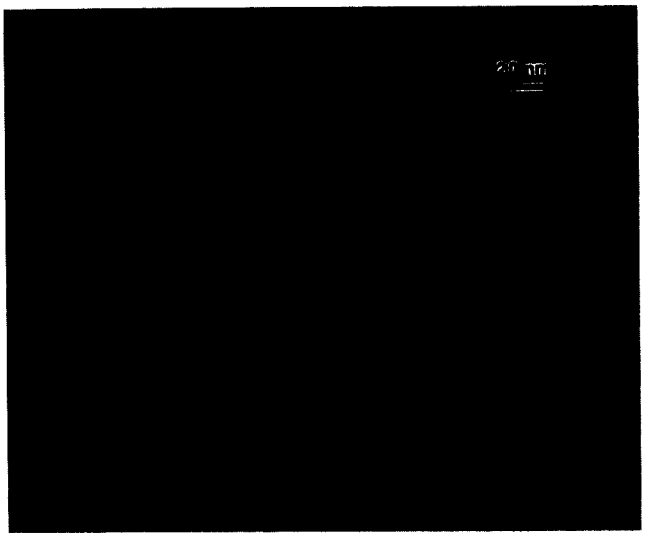

Fig. 7. TEM of $[(C_2H_4)_2RhOEt]_2$ solution after photolysis for 25 min.

On one area of the grid, a large particle was found which was approximately the same size (200 nm) as the particles removed from the walls of the reaction vessel and characterized by SEM. This larger particle gave a more intense electron diffraction pattern consisting of one diffuse ring, again consistent with the most intense diffraction line of FCC rhodium. The broadening of the electron diffraction pattern is approximately consistent with the presence of crystalline rhodium with a crystallite size of about 20–30 Å. EDS revealed that rhodium was present both in the small and large particles. No evidence for Rh_2O_3 was observed.

In a larger scale experiment, 0.060 g (0.147 mmol) of $[(C_2H_4)_2RhOEt]_2 \cdot H_2O$ was dissolved in 10 ml of benzene in a 50 ml Schlenk flask. Then the solution was irradiated with a mercury lamp for 4 h at room temperature. After removing the solvent *in vacuo*, black air-sensitive and pyrophoric agglomerates were obtained. X-ray powder diffraction of this sample showed the presence of a broad peak corresponding to a d-spacing of ~ 2.2 Å. After heating to 400°C *in vacuo*, the peaks sharpened and revealed only the presence of Rh.

4. Conclusions

Thermogravimetric analyses of the series of compounds $[L_2RhCl]_2$, where $L_2 = 1,5\text{-COD,NBD}$ and $(C_2H_4)_2$ under air, nitrogen and 7% H_2 in N_2 atmospheres reveal that thermal decomposition behavior depends on the nature of the olefin ligand and the composition of the atmosphere. Under a 7% H_2 in N_2 atmosphere, the onset of thermal decomposition of

these species occurs in the following order: $L_2 = (C_2H_4)_2$, 91°C; NBD, 143°C; 1,5-COD, 212°C. Under a nitrogen atmosphere, $[L_2RhCl]_2$, L_2 = NBD and $(C_2H_4)_2$, undergo weight loss consistent with loss of one or more olefin ligands, then formation of Rh metal at higher temperatures. In contrast, $[(1,5\text{-COD})RhCl]_2$ formed Rh metal directly. In air, thermal decomposition generally resulted in formation of crystalline Rh metal followed by oxidation above 500°C to form crystalline Rh_2O_3, except for $[(C_2H_4)_2RhCl]_2$, which gave Rh_2O_3 directly. In some experiments, a weight loss consistent with formation of "RhCl" was observed. However, as a result of the crystalline Rh present, it is proposed that disproportionation to Rh and $RhCl_3$ may have occurred.

The species $[L_2RhCl]_2$, L_2 = 1,5-COD and NBD, do not decompose on irradiation with a Hg lamp. However, whereas $[(C_2H_4)_2RhCl]_2$ undergoes slow decomposition, $[(C_2H_4)_2Rh(OEt)]_2 \cdot H_2O$ undergoes rapid photochemical decomposition to give crystalline Rh with a small (2 nm) crystallite size. It is not clear whether the lability of the alkoxide derivative compared to the chloride derivative is a result of the greater lability of the metal–olefin bond in the alkoxide compound or the greater lability of the ethoxide ligand compared to chloride.

These studies will aid in the proper choice of ligands and processing conditions for the formation of highly dispersed Rh particles [26]. Further experiments are in progress to probe the disproportionation of Rh^1 compounds as a method of formation of Rh metal.

Acknowledgments

MHS thanks the Johnson-Matthey precious metals loan program for loan of $RhCl_3 \cdot 3H_2O$ and U.S. DOE under contract number DE-AC04-76DP00789 through Pittsburgh Energy Technology Center. We thank Prof A. Datye for TEM measurements, John Garvey for SEM measurements and Dr. Y. Shin for X-ray powder diffraction measurements. M.H.-S. thanks the NSF Chemical Instrumentation program for the purchase of a low-field NMR spectrometer.

References

1 K. Klabunde, Y.-X. Li and B.-J. Tan, *Chem. Mater., 3* (1991) 30.
2 R. C. Davis and K. Klabunde, *J. Chem. Rev., 82* (1982) 152.
3 B. C. Gates, in L. L. Hegedus (ed.), *Catalyst Design, Progress and Perspectives*, John Wiley and Sons, New York, 1987.
4 I. M. Campbell, in *Catalysis at Surfaces*, Chapman and Hall, New York, 1988.
5 See e.g. B. Breitscheidel, J. Zieder and U. Schubert, *Chem. Mater., 3* (1991) 559, and references therein.
6 S. Poston and A. Reisman, *J. Electron. Mater., 18* (1989) 553.
7 M. Che and C. O. Bennett, in D. D. Eley, H. Pines and P. B. Weisz (eds.), *Advances in Catalysis, 36* (1989) 55, Academic Press, New York.
8 C. J. Brinker and G. W. Scherer, *Sol-Gel Science, The Physics and Chemistry of Sol-Gel Processing*, Academic Press, 1990.
9 B. C. Gates, in *Catalytic Chemistry*, John Wiley and Sons, New York, 1992.
10 T. A. Wark, E. A. Gulliver, M. J. Hampden-Smith and A. L. Rheingold, *Inorg. Chem., 29* (1990) 4360.
11 S. L. Anderson, A. K. Datye, T. A. Wark and M. J. Hampden-Smith, *Catal. Lett., 8* (1991) 345.
12 Z. Duan, M. J. Hampden-Smith and A. Sylwester, *Chem. Mater.*, 1992, in press.
13 Z. Duan, M. J. Hampden-Smith and A. Datye, in *Chemical Processes in Inorganic Materials: Metal and Semiconductor Clusters and Colloids, Mat. Res. Soc. Symp. Proc.*, 1992, in press.
14 H. D. Kaesz, R. S. Williams, R. E. Hicks, Y. J. A. Chen, S. Xue, D. Xu, D. K. Shuh and H. Thridandam, *Mat. Res. Soc. Symp. Proc., 131* (1989) 395.
15 A. Etspuler and H. Suhr, *Appl. Phys. A., 48* (1989) 373.
16 D. C. Smith, S. G. Pattillo, N. E. Elliot, T. G. Zocco, C. J. Burns, J. R. Laia and A. P. Sattleberger, *Mat. Res. Soc. Symp. Proc., 168* (1990) 369.
17 D. F. Shriver and M. A. Drezden, *The Manipulation of Air-Sensitive Compounds*, 2nd edition, Wiley-Interscience, New York, 1986, p. 78.
18 G. Giordano and R. H. Crabtree, *Inorg. Synth., 28* (1990) 88.
19 E. W. Abel, M. A. Bennett and G. Wilkinson, *J. Chem. Soc.*, (1959) 3178.
20 R. Cramer, *Inorg. Synth., 28* (1990) 86.
21 R. Cramer, *Inorg. Chem., 1* (1962) 722.
22 R. Cramer, *J. Am. Chem. Soc., 86* (1964) 217.
23 J. Sandstrom, *Dynamic NMR Spectroscopy*, Academic Press, London, 1982.
24 P. Doppelt, V. Weigel and P. Guinot, *Proceedings of the European Materials Research Society, Strasbourg, June, 1992.*
25 E. S. Freeman and B. Carroll, *J. Phys. Chem., 62* (1958) 394.
26 A. S. Gurav, Z. Duan, L. Wang, M. J. Hampden-Smith and T. T. Kodas, *Chem. Mater.*, 1993, in press.